BIOCHEMISTRY
including biophysical chemistry & molecular biology
Article

Biochemistry **2010,** *49,* 10081–10088 10081
DOI: 10.1021/bi1009997

A Specific Interaction of L-Tryptophan with CO of CO-Bound Indoleamine 2,3-Dioxygenase Identified by Resonance Raman Spectroscopy†

Sachiko Yanagisawa,‡ Hiroshi Sugimoto,§ Yoshitsugu Shiro,§ and Takashi Ogura*,‡

‡*Department of Life Science and Picobiology Institute, Graduate School of Life Science, University of Hyogo, Koto 3-2-1, Kamigori-cho, Ako-gun, Hyogo 678-1297, Japan, and* §*Biometal Science Laboratory, RIKEN SPring-8 Center, Koto 1-1-1, Sayo-cho, Sayo-gun, Hyogo 679-5148, Japan*

Received June 21, 2010; Revised Manuscript Received October 27, 2010

ABSTRACT: Indoleamine 2,3-dioxygenase (IDO) is a heme enzyme which catalyzes dioxygenation of L-Trp (tryptophan), yielding *N*-formylkynurenine. IDO thus plays a key role in L-Trp catabolism in mammals. In the present study, resonance Raman (RR) spectra of the reduced carbon monoxide- (CO-) bound form of IDO were measured in order to gain insights into the active site environment of O_2. Binding of CO to L-Trp-bound IDO causes a significant change in the electronic and RR spectra of the heme, indicating that the π^* orbitals of the carbon atom of CO interact with π orbitals of Fe and the porphyrin. On the other hand, binding of CO to D-Trp-bound IDO does not induce the same change. This is also the case with substrate-free IDO. Based on the distinct absorption spectra and RR bands of the vibrational signature of CO (ν(CO), δ(FeCO), and ν(Fe−CO)) of the L-Trp-bound species relative to the other two species, it is confirmed that sterically constrained geometry of the Fe−O−O unit exists as previously reported (Terentis, A. C., et al. (2002) *J. Biol. Chem. 277*, 15788−15794). In contrast, binding of D-Trp does not induce such constraint. The comparable values of V_{max} reported for L-Trp and D-Trp are interpreted as a result of a change in the rate-limiting step in the reaction cycle of the enzyme induced by the D-enantiomer relative to the L-enantiomer. Enhancements of the overtone and the combination Raman modes of the Fe−CO stretching vibration are evident. The anharmonicity of the Fe−CO stretching oscillator is significantly higher than those of oxygen carrier proteins. This is a specific character of IDO and might be responsible for the unique reactivity of this enzyme.

Indoleamine 2,3-dioxygenase (IDO)[1] is a heme enzyme found in all mammalian tissues with the exception of liver (*1*). This enzyme catalyzes the first step of the kynurenine pathway, which is the main catabolic pathway of tryptophan (Trp) (*2*, *3*). In the reaction, two oxygen atoms are incorporated into Trp, yielding *N*-formylkynurenine. Recent biomedical studies have suggested that catabolic activity of the kynurenine pathway is implicated in immune system disturbances (*4*), neural disorders (*5*), tumor immunoediting processes (*6*), regulation of T cell immunity (*7*), and other conditions. IDO has attracted considerable attention from biochemists, biophysicists, spectroscopists, and physicians.

The IDO reaction was thought to depend upon a basic functional group interacting with the NH of Trp to initiate the proton abstraction step of the reaction (*8*). However, the 2.3 Å crystal structure of the 4-phenylimidazole-bound derivative of IDO indicates that such an interaction does not exist (*9*). Based on these results, a reaction mechanism was presented in which the iron-bound oxygen abstracts the proton. In most reaction mechanisms suggested thus far, two oxygen atoms of dioxygen are incorporated into Trp without immediate cleavage of the O−O bond (*9*). However, recent resonance Raman (RR) studies have revealed the existence of a Fe^{IV}=O-type heme species during catalytic turnover, which was quite unexpected (*10*, *11*). This indicates that O−O bond cleavage takes place during the oxygenation reaction. A recent theoretical investigation supports this mechanism (*12*). It is known that L-Trp ((*S*)-Trp) is a better substrate for IDO than D-Trp ((*R*)-Trp). The K_m value for L-Trp is significantly smaller than that of D-Trp. On the other hand, it has been reported that the V_{max} values for the IDO reaction with L-Trp and with D-Trp are similar (*13*). This means that although IDO favors binding of L-Trp over D-Trp due to steric effects, it reacts with both enantiomers at similar rates.

In the present study, we employ carbon monoxide (CO) as a probe to examine the interaction between the substrate and CO in the IDO-Trp-CO ternary complex for the two Trp enantiomers. RR results reveal that CO is affected by the distinct active site environments which are generated upon binding of each of the two Trp enantiomers. An interaction mode specific to L-Trp is evident in the absorption and RR spectra.

MATERIALS AND METHODS

Recombinant human IDO was expressed in *Escherichia coli* and purified as previously reported (*9*). A protein solution was prepared in 50 mM potassium phosphate buffer, pH 6.5. CO-bound forms of IDO were prepared by addition of $Na_2S_2O_4$ (to a

†This work was supported by a Grant-in-Aid for Scientific Research (C) (No. 21570171) and Priority Area (Molecular Science for Supra Functional Systems, No. 477) (No. 20050029) to T.O. and by the GCOE program "Picobiology: Life Science at Atomic Level" at the Graduate School of Life Science, University of Hyogo. S.Y. is a recipient of a Young Scientist Research Fellowship from JSPS.

*To whom correspondence should be addressed. Phone: +81-791-58-0181. Fax: +81-791-58-0182. E-mail: ogura@sci.u-hyogo.ac.jp.

[1]Abbreviations: IDO-(D-Trp)-CO, D-Trp-bound IDO-CO; IDO-(L-Trp)-CO, L-Trp-bound IDO-CO; IDO-CO, carbon monoxide-bound IDO (substrate free); IDO, indoleamine 2,3-dioxygenase; RR, resonance Raman; ν(CO), C−O stretching mode; ν(Fe−CO), Fe−CO stretching mode; δ(FeCO), Fe−C−O bending mode.

Published on Web 10/28/2010

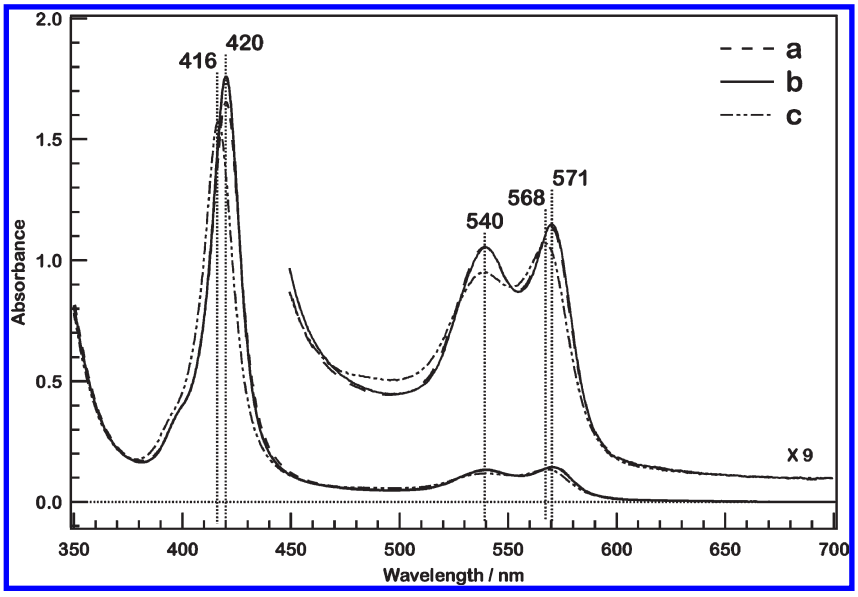

FIGURE 1: Absorption spectra of CO-bound IDO with 30 mM D-Trp (a), without Trp (b), and with 10 mM L-Trp (c). The concentration of IDO was 30 μM.

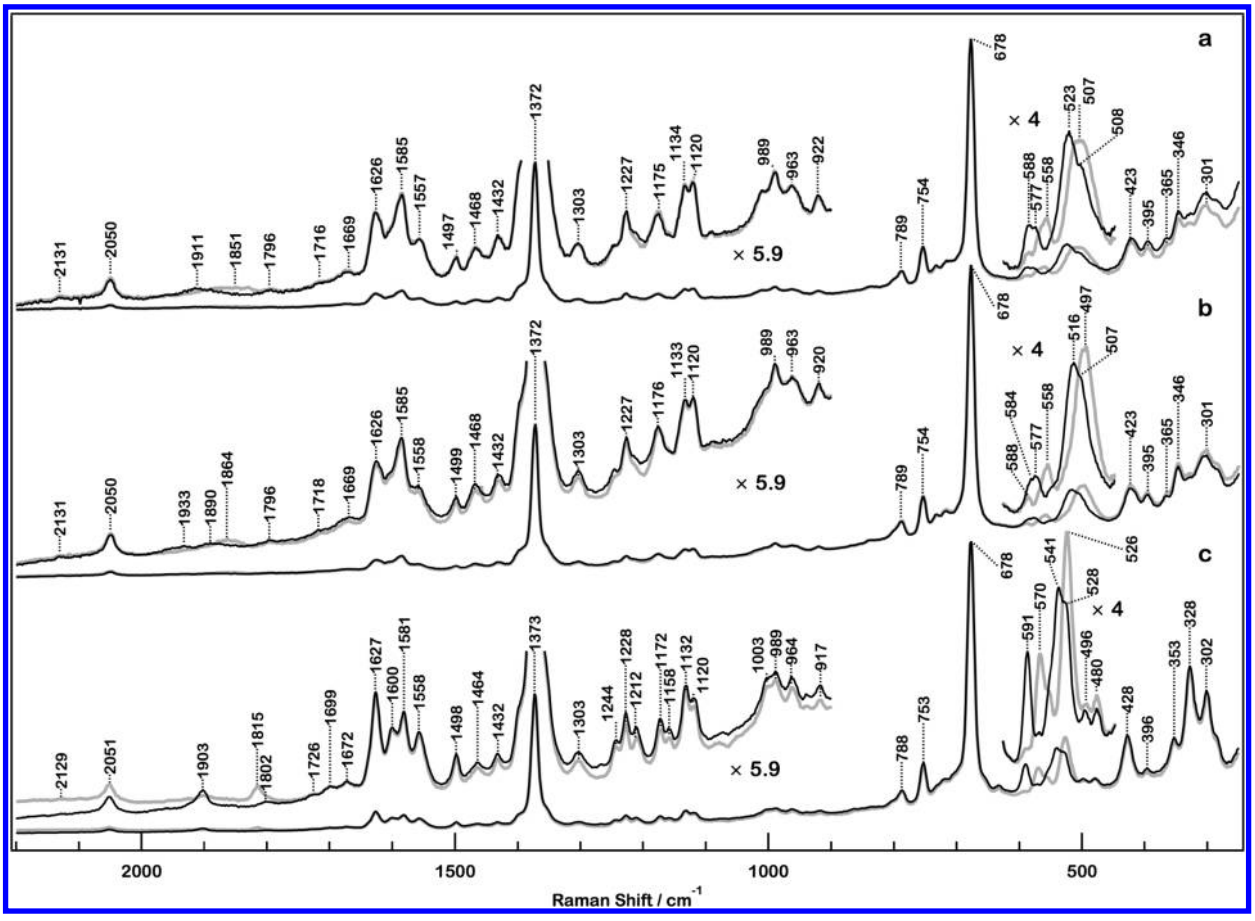

FIGURE 2: Resonance Raman spectra of IDO-(D-Trp)-CO (a), IDO-CO (b), and IDO-(L-Trp)-CO (c). Light-colored spectra are for corresponding $^{13}C^{18}O$ adducts. The concentration of IDO was 30 μM. The accumulation time for Raman scattering data was 60 min for spectra a and b and 90 min for spectrum c.

final concentration of 5 mM) to solutions of ferric IDO containing 10 mM L-Trp, 0 mM Trp, and 30 mM D-Trp under a $^{12}C^{16}O$ or $^{13}C^{18}O$ atmosphere. The known concentrations of the L-Trp and D-Trp solutions were used to prepare the fully bound form as determined by absorption and RR spectra. Raman scattering of the sample was measured in a cylindrical spinning cell (inner diameter = 3 mm) at 2400 rpm with excitation at 413.1 nm by a Kr^+ laser (Spectra Physics, Model 2060). Laser power of 125 μW at the sample was chosen to minimize photodissociation of CO. The detector was a liquid nitrogen-cooled CCD (Roper Scientific, Spec-10: 400B/LN) attached to a single polychromator (Chromex, 500IS) as described previously (*11*). The spectral slit

width was 8 cm^{-1}. Raman shifts were calibrated with indene as the frequency standard. The accuracy of Raman shifts is ± 1 cm^{-1} for an isolated intense band. Absorption spectra of the samples in the spinning cell were measured with a spectrophotometer (Hitachi, U3310) using a custom-built attachment to fit the spinning cell to an ordinary cuvette holder. This arrangement enables us to verify the integrity of the samples before and after the RR measurements are made. The absorption spectra in Figure 1 were measured using a cuvette with a 3 mm light path.

RESULTS

Figure 1 depicts absorption spectra of CO-bound IDO in the presence of D-Trp (a), in the absence of Trp (b), and in the presence of L-Trp (c). We note that IDO-(D-Trp)-CO (Figure 1a) and IDO-CO (substrate-free) (Figure 1b) exhibit Soret-, β-, and α-band absorption maxima at the same positions (420, 540, and 571 nm, respectively), and these spectra are identical with the exception of a slight variation in intensity at 420 nm. This indicates that the electronic structures of the heme in the two species are very similar. On the other hand, blue-shifted Soret- and α-band maxima at 416 and 568 nm of IDO-(L-Trp)-CO (Figure 1c) relative to those of IDO-(D-Trp)-CO and IDO-CO are evident, indicating that the electronic structure of the heme in IDO-(L-Trp)-CO is distinct.

Figure 2 depicts RR spectra of IDO-(D-Trp)-CO (a), IDO-CO (b), and IDO-(L-Trp)-CO (c). These spectra correspond to the absorption spectra shown in Figure 1 in the region between 250 and 2200 cm^{-1}. The light-colored RR spectra are for the $^{13}C^{18}O$ isotopomers. The position of the ν_4 mode (an oxidation state marker) at 1372 cm^{-1} (a), 1372 cm^{-1} (b), and 1373 cm^{-1} (c) is consistent with the expected positions of this band for CO adducts. The bands that exhibit an apparent $^{13}C^{18}O$ isotopic frequency shift in the ca. 2000−1900 and 600−500 cm^{-1} regions are vibrational modes of CO, which will be discussed in detail. The spectral patterns (with the exception of the bands corresponding to the CO-related modes shown in Figures 2a and 2b, as discussed above) are identical and distinct from the spectral pattern shown in Figure 2c, where the following differences are evident; there is a new band at 328 cm^{-1}, which is assignable to an out-of-plane γ_6 mode (*14*), there is intensification of the bands at 428, 1003, 1158, 1212, 1498, 1600, and 1627 cm^{-1}, and there is a change in the relative intensities of the bands at 1132 and 1120 cm^{-1}. The bands at 428 and 1627 cm^{-1} are assignable to the bending and C=C stretching modes, respectively, of the vinyl substituents of the porphyrin. The intensification of these bands indicates the occurrence of a conformational change of the vinyl substituents (*15*). The ν_3 mode (a marker for the coordination number of the heme) is identified at essentially the same frequency at 1497, 1499, and 1498 cm^{-1} in Figures 2a, 2b, and 2c, respectively, and is consistent with a 6-coordinate heme. The ν_2 mode (a spin state marker of the heme) is located at 1585 cm^{-1} for IDO-(D-Trp)-CO and IDO-CO and at 1581 cm^{-1} for IDO-(L-Trp)-CO. These values are consistent with a low-spin complex. However, the 4 cm^{-1} lower frequency of the L-Trp complex relative to that of the other two species indicates that the porphyrin core has expanded slightly. The mode at 1626 cm^{-1} for IDO-(D-Trp)-CO and IDO-CO is assignable to the $\nu_{C=C}$ mode of the heme peripheral substituent. Although the frequency difference of the mode at 1627 cm^{-1} for IDO-(L-Trp)-CO is insignificant, a significant intensification of the band (Figure 2c) is an indication of the change in electronic and geometric

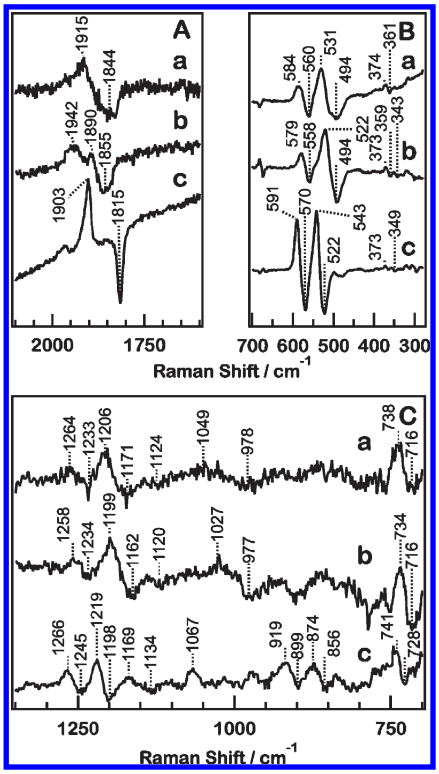

FIGURE 3: Resonance Raman isotopic difference spectra ($^{12}C^{16}O$ minus $^{13}C^{18}O$) of three kinds of IDO-CO species. Panels A, B, and C are for regions 2100−1600 cm^{-1}, 700−280 cm^{-1}, and 1350−700 cm^{-1}, respectively. (a) IDO-(D-Trp)-CO, (b) IDO-CO, and (c) IDO-(L-Trp)-CO. These isotopic difference spectra are calculated from the raw spectra shown in Figure 2. Frequencies shown are apparent readings of the Raman difference spectra and thus may be slightly different from those in Tables 1 and 2 obtained after fitting simulations.

structures of the porphyrin vinyl groups in the L-Trp complex. The band at 2050 cm^{-1} is readily assignable to the combination of the ν_4 mode (1372 cm^{-1}) and the ν_7 mode (678 cm^{-1}), since the sum of the two frequencies is equivalent to 2050 cm^{-1}. There are shoulders on the lower frequency side of the ν(Fe−CO) (Fe−CO stretching) bands at 523, 516, and 541 cm^{-1}, which are located approximately at 508, 507, and 528 cm^{-1}. As will be discussed below, the former three bands exhibit CO-isotope sensitivity, but the latter three do not. This indicates that the latter three bands originate from porphyrin vibrations.

Figure 3 depicts isotopic difference RR spectra for regions between 1600 and 2100 cm^{-1} (panel A), 280 and 700 cm^{-1} (panel B), and 700 and 1350 cm^{-1} (panel C) obtained by subtracting RR spectra for $^{13}C^{18}O$ from those for $^{12}C^{16}O$, which are shown in Figure 2. The RR spectra a, b, and c in panels A, B, and C are for IDO-(D-Trp)-CO, IDO-CO, and IDO-(L-Trp)-CO, respectively. Band intensities, widths, and positions have been determined by fitting simulations under the assumption that the observed Raman bands are of Gaussian band shape. Figure 4 depicts examples of fitting simulations for isotopic Raman difference ($^{12}C^{16}O - {}^{13}C^{18}O$) spectra for IDO-(L-Trp)-CO. Panels A, B, and C are for the 1700−2100, 400−700, and 670−1350 cm^{-1} regions, respectively. Spectral series a represents simulated Gaussian curves. Spectral series b represents the sum of simulated Gaussian curves. Spectral series c represents the experimentally obtained isotopic difference spectra (the same series as spectral series c in Figure 3 but with the linear baseline subtracted if necessary). Spectral series d represents the residual spectra obtained by subtracting individual spectra of spectral series b from individual

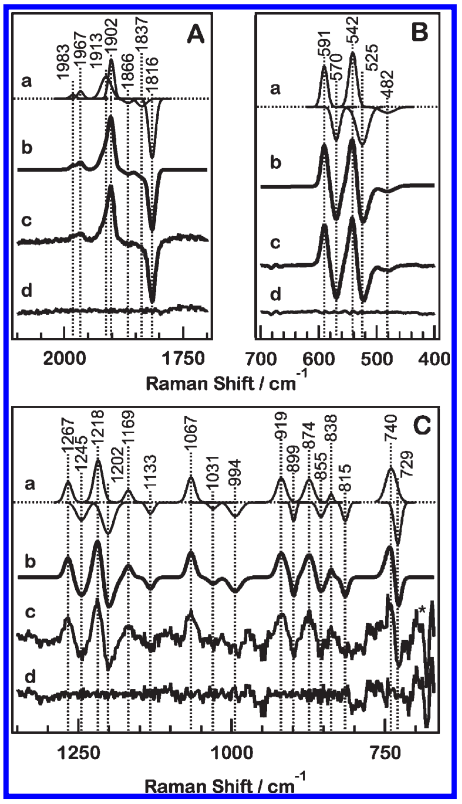

FIGURE 4: Results of fitting simulations for isotopic difference RR spectra for IDO-(L-Trp)-CO species. Panels A, B, and C are for regions 2100−1700 cm^{-1}, 700−400 cm^{-1}, and 1350−670 cm^{-1}, respectively. (a) Simulated individual Gaussian curves, (b) sum of the Gaussian curves in (a), (c) experimentally obtained difference spectrum from Figure 3-c, whose linear baseline has been subtracted, and (d) the residual spectrum obtained by subtracting spectrum b from spectrum c. Panels B and C are versions obtained for different wavenumber regions. The difference feature marked with an asterisk is due to incomplete cancellation of a very intense Raman band and is not caused by a CO-isotope shift.

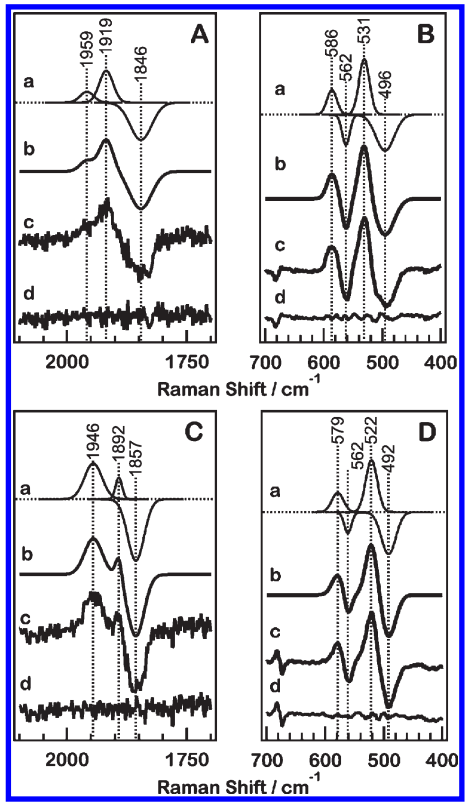

FIGURE 5: IDO-(D-Trp)-CO (A and B) and IDO-CO (C and D) versions of Figure 4. The 700−1350 cm^{-1} region is not shown.

spectra of spectral series c. The flat features of spectral series d show excellent fit with the individual spectra shown in panels A, B, and C. The same sets of spectra in the 1700−2100 and 400−700 cm^{-1} regions for IDO-CO and IDO-(D-Trp)-CO are shown in Figure 5. Table 1 summarizes the Raman frequencies based on the fitting simulations shown in Figures 4 and 5 with their vibrational assignments. Table 2 summarizes the details of the fitting simulations for the ν(CO) (C−O stretching) band.

In Figure 3, the most apparent difference among the IDO-(D-Trp)-CO, IDO-CO, and IDO-(L-Trp)-CO species is found in the frequency of the ν(CO) mode region at 1915/1844, 1942 and 1890/1855, and 1903/1815 cm^{-1} for $^{12}C^{16}O/^{13}C^{18}O$. The ν(CO) mode of IDO-CO was not observed in the previous report (*15*). However, in the present study, the existence of the band is evident in spectrum b in panel A of Figure 3. It is likely that CO is most easily photodissociated in the substrate-free state under the previously adopted experimental conditions. The ν(CO) frequency of the three species is distinct, and we note that the bandwidth for IDO-(L-Trp)-CO is significantly narrower than those of the other two species, indicating the existence of a sterically constrained conformer. We observed the ν(Fe−CO) mode at 531/496, 522/492, and 542/525 cm^{-1} for the $^{12}C^{16}O/^{13}C^{18}O$ isotopomers for IDO-(D-Trp)-CO, IDO-CO, and IDO-(L-Trp)-CO (Figures 4B and 5B,D). We can identify another prominent isotopic shift in the Raman bands in the 591−562 cm^{-1} region and assign this band to the δ(FeCO) (FeCO bending) mode (*16*, *17*). Fitting simulations showed that the frequency of the δ(FeCO) band is 586/562, 579/562, and 591/570 cm^{-1} for IDO-(D-Trp), IDO-CO, and IDO-(L-Trp)-CO, respectively, for the $^{12}C^{16}O/^{13}C^{18}O$ isotopomers. We note that there is significant enhancement of the band for IDO-(L-Trp)-CO at 591/570 cm^{-1} (Figure 3B, spectrum c). The concentration of L-Trp (10 mM) used was the concentration at which substrate inhibition takes place (*18*). We carefully examined the region of the ν(Fe−CO) mode of the RR spectra for L-Trp concentrations of 100 μM (data not shown) and for 10 mM concentrations and confirmed that for both concentrations of Trp there was only a single band assignable to the ν(Fe−CO) mode at 542 cm^{-1}. This indicates that IDO-(L-Trp)-CO exhibits a single ν(Fe−CO) band at L-Trp concentrations of 100 μM and 10 mM. We also observed the heme deformation mode (*16*) at 374/361, 373/351, and 373/349 cm^{-1} for the three species (Table 1). This mode indicates sensitivity to the CO isotope. We have not performed the fitting analyses for this mode due to the weak intensity of the difference features in the isotopic difference spectra (Figure 3B). Therefore, the frequency of this mode should contain larger error. In addition to these modes, we identified an isotopic difference pattern in Figure 4C in the 700−1350 cm^{-1} region at 1267/1245, 1218/1202, 1169/1133, 1067/(not observed), 919/899, 874/855, and 740/729 cm^{-1} for the $^{12}C^{16}O/^{13}C^{18}O$ isotopomers for IDO-(L-Trp)-CO. We have performed fitting simulations with respect to these modes as exemplified in Figure 4 and assigned the Raman bands to ν_7 + δ(FeCO), ν_7 + ν(Fe−CO), 2δ(FeCO), 2ν(Fe−CO), γ_6 + δ-(FeCO), γ_6 + ν(Fe−CO), and ν(Fe−CO) + ν(Fe−His) (*16*). These assignments are summarized in Table 1.

DISCUSSION

The ν(CO) Frequency of the $^{12}C^{16}O$ Species. Each of the three species (IDO-(L-Trp)-CO, IDO-CO, and IDO-(D-Trp)-CO)

Table 1: CO-Isotope-Sensitive Raman Frequencies for $^{12}C^{16}O/^{13}C^{18}O$ Isotopomers[a]

	Raman shift/cm^{-1}					
	ν(CO)	$\nu_7 + \delta$(FeCO)	$\nu_7 + \nu$(Fe−CO)	2δ(FeCO)	2ν(Fe−CO)	$\gamma_6 + \delta$(FeCO)
D-Trp	1959·1919/1846	1263/1234	1207/1173	no[b]/1126	1053/979	no[b]/no[b]
no Trp	1946/1857	1252/1237	1197/1164	no[b]/1120	1023/972	no[b]/no[b]
L-Trp	1913·1902/1816	1267/1245	1218/1202	1169/1133	1067/no[b]	919/899

	Raman shift/cm^{-1}						
	$\gamma_6 + \nu$(Fe−CO)	ν(Fe−CO) + ν(Fe−His)[c]	δ(FeCO)	ν(Fe−CO)	δheme[d]	$\nu_7^{obs\,e}$	$\gamma_6^{obs\,e}$
D-Trp	no[b]/no[b]	738/715	586/562	531/496	374/361	678	no[b]
no Trp	no[b]/no[b]	734/716	579/562	522/492	373/351	678	no[b]
L-Trp	874/855	740/729	591/570	542/525	373/349	678	328

[a]Vibrational frequencies of CO-isotope-sensitive Raman bands with their assignments. The frequencies of Raman bands were determined by fitting simulations shown in Figures 4 and 5 and are rounded off to the least significant digit. The ν(CO), δ(FeCO), δheme, and ν(Fe−CO) denote the C−O stretching mode, the FeCO bending mode, the heme deformation mode, and the Fe−CO stretching mode, respectively. [b]no: not observed. [c]Assignment according to ref *16*. The ν(Fe−His) mode is located at approximately 200 cm^{-1}. [d]CO-isotope-sensitive heme deformation mode. Assignment according to ref *16*. [e]Frequencies from Figure 2.

measured in the present study show two positive Raman bands for $^{12}C^{16}O$ but only one negative Raman band for $^{13}C^{18}O$ in the ν(CO) frequency region of the isotopic difference spectra (Figures 4 and 5). The IDO-(L-Trp)-CO spectrum exhibits the two bands at 1913 and 1902 cm^{-1} for $^{12}C^{16}O$ and one band at 1816 cm^{-1} for $^{13}C^{18}O$. The relative intensities of the two former Raman bands are identical as shown in Table 2. If there are two conformers, both of the $^{12}C^{16}O$ and the $^{13}C^{18}O$ isotopomers would be expected to have two ν(CO) modes, but this is not the case. Instead, our interpretation is that there is one conformer that gives an intermediate frequency at 1908 cm^{-1} for $^{12}C^{16}O$. This band splits into two bands as a result of an incidental interaction with another oscillator at a similar frequency. The combination of the ν_4 mode at 1373 cm^{-1} with the ν(Fe−CO) mode at 542 cm^{-1}, which is silent in the RR spectrum, may be responsible (1373 + 542 = 1915). Under an approximation of the C−O harmonic oscillator, the reduced masses of $^{12}C^{16}O$ and $^{13}C^{18}O$ are calculated to be 6.857 and 7.548 amu, respectively. The isotopic shift of the ν(CO) frequency can be estimated as 1823 and 1813 cm^{-1} at the lowest for the 1913 and 1902 cm^{-1} species, respectively, upon replacement of $^{12}C^{16}O$ with $^{13}C^{18}O$. These are the lowest limits assuming that the RR band has 100% C−O stretching character. We locate the ν(CO) frequency at 1908 cm^{-1}, which is the average frequency of 1913 and 1902 cm^{-1}, as stated above. The observed ν(CO) frequency for $^{13}C^{18}O$ is 1816 cm^{-1} and an intermediate frequency of 1823 and 1813 cm^{-1}.

The IDO-(D-Trp)-CO species also exhibits the two ν(CO) bands at 1959 and 1919 cm^{-1} for $^{12}C^{16}O$ and one at 1846 cm^{-1} for $^{13}C^{18}O$ (Table 2). Similarly, for IDO-(L-Trp)-CO, we located a single ν(CO) mode at 1939 cm^{-1} which represents an intermediate frequency between the 1959 and 1919 cm^{-1} (Figure 5A-a) bands. These two bands have similar band widths of 20.1 and 20.3 cm^{-1}, respectively.

In the case of the absence of Trp, there are also two bands at 1946 and 1892 cm^{-1} for $^{12}C^{16}O$ and one band at 1857 cm^{-1} for $^{13}C^{18}O$ (Table 2, Figure 5). In this case, it is likely that the band at 1892 cm^{-1} represents a combination of the ν_4 mode at 1372 cm^{-1} and the ν(CO) mode at 522 cm^{-1} (1372 cm^{-1} + 522 cm^{-1} = 1894 cm^{-1}). The Raman band originating from the combination mode ($\nu_4 + \nu_{Fe-C}$) was detected at 1885 cm^{-1} for cytochrome *c* oxidase (S. Yanagisawa and T. Ogura, unpublished observations). The degree of enhancement of the combination mode depends upon the anharmonicity of the Fe−CO oscillator (*vide infra*). The bandwidths of the 1946 and the 1857 cm^{-1} bands are 25.7 and 24.2 cm^{-1}, respectively. Although the previous report failed to observe the ν(CO) mode in the absence of Trp (most likely as a result of photodissociation) (*15*), it is observed in the present study.

Table 2: Analyses of the ν(CO) Bands in Figures 4 and 5[a]

D-Trp	frequency	1958.8	1918.6	1846.2
	width	20.1	20.3	31.7
	relative intensity	0.1142	0.3391	0.6250
no Trp	frequency	1945.6	1892.3	1856.7
	width	25.7	9.5	24.2
	relative intensity	0.3545	0.0792	0.5733
L-Trp	frequency	1912.7	1901.7	1815.6
	width	15.0	8.3	10.0
	relative intensity	1.244	1.224	2.230

[a]Numerical data showing the results of fitting simulations shown in Figures 4 and 5 for the bands in the ν(CO) region. Simulated bands, bandwidths, and relative intensities are shown. Relative intensity is expressed as calculated area of a simulated Raman band. Units for frequency and width are in cm^{-1}.

Table 3 summarizes the estimated ν(CO) frequencies for the IDO-(L-Trp)-CO, IDO-CO, and IDO-(D-Trp)-CO species prepared with $^{12}C^{16}O$ based on the discussion above. The shift values ($\Delta(^{13}C^{18}O)$) for IDO-(L-Trp)-CO, IDO-CO, and IDO-(D-Trp)-CO upon replacement with $^{13}C^{18}O$ are −92, −89, and −93 cm^{-1}, respectively (Table 3). It is known that there is a linear inverse relationship known as the back-bonding correlation between ν(CO) and ν(Fe−CO) for different types of CO-bound hemoproteins (*19*−*22*). When the corresponding data of the three different CO derivatives of IDO are placed in a plot of ν(CO) vs ν(Fe−CO), the resulting linear relationship is similar to the relationship observed for hemoproteins with histidine-ligated protoheme. IDO-(L-Trp)-CO is located at a position close to that of horseradish peroxidase (ν_{CO} = 1904 cm^{-1} and ν_{Fe-CO} = 537 cm^{-1}) (*23*−*25*) and hemoglobin from *Ascaris* nematode (ν_{CO} = 1909 cm^{-1} and ν_{Fe-CO} = 543 cm^{-1}) (*26*).

Active Site Environment. The ν(CO) and the ν(Fe−CO) frequencies are different for the three species, and accordingly, the frequencies of the overtone and combination bands are different as shown in Table 1. The observation of both the fundamental and the first overtone of the ν(Fe−CO) mode at 542/1067, 522/1023, and 531/1053 cm^{-1} for the IDO-(L-Trp)-CO,

Table 3: Estimated ν(CO) Frequencies (See Text)[a]

	ν(CO) ($^{12}C^{16}O/^{13}C^{18}O$)/cm^{-1}	$\Delta\nu(^{13}C^{18}O)$/cm^{-1}
D-Trp	1939/1846	−93
no Trp	1946/1857	−89
L-Trp	1908/1816	−92

[a]The estimated true ν(CO) frequencies for $^{12}C^{16}O/^{13}C^{18}O$ for IDO-(D-Trp)-CO, IDO-CO, and IDO-(L-Trp)-CO and their shift values ($\Delta(^{12}C^{16}O/^{13}C^{18}O)$) which occur upon isotopic substitution.

IDO-CO, and IDO-(D-Trp)-CO species, respectively, have allowed us to calculate the anharmonic constant (χ). Here, the expected frequencies for the fundamental and overtone in the presence of anharmonicity are $\nu_e(1 - 2\chi)$ and $2\nu_e(1 - 3\chi)$ (*27*). The obtained values for IDO-(L-Trp)-CO, IDO-CO, and IDO-(D-Trp)-CO are 0.014, 0.015, and 0.015, respectively. These values represent the averages of two independent experiments. The values are identical for the three species. We note that these values are significantly higher than those of myoglobin (0.008) and hemoglobin (0.010) (*27*) and those of other hemoproteins (*28*). Anharmonicity of an oscillator is a result of distortion of the potential curve in which the oscillator vibrates. The anharmonicity observed for the Fe−CO oscillator of IDO in the present study is 2-fold higher than that of oxygen carriers and has almost the same value for IDO with bound L-Trp, bound D-Trp, and in the absence of Trp. This means that the characteristics of the heme pocket environment which provide anharmonicity to the Fe−CO oscillator are intrinsic and not induced by binding of substrate. A clear difference between the heme pocket structures of oxygen carriers and IDO is that the distal histidine which is present in the oxygen carriers is missing in IDO. A higher degree of anharmonicity facilitates mixing of vibrations of more than one oscillator, and this might be related to the specific reaction mechanism of IDO. Detectability of a combination mode ($\nu_4 + \nu_{Fe-CO}$) at 1892 cm^{-1} might be a result of the high degree of anharmonicity. Notably, a similar combination mode was detectable for bovine heart cytochrome *c* oxidase at 1885 cm^{-1}. The anharmonicity observed for cytochrome *c* oxidase is estimated to be 0.012, which is an intermediate value between those of the oxygen carriers and IDO. The higher anharmonicity identified for IDO compared to that of oxygen carriers is a specific character of this enzyme and might be responsible for the unique reactivity of this enzyme.

The bandwidth of the ν(CO) mode for IDO-(L-Trp)-CO is ca. 10 cm^{-1}. This is significantly smaller than that of IDO-CO (ca. 24 cm^{-1}) and IDO-(D-Trp)-CO (ca. 32 cm^{-1}) which are shown in Figure 3 and Table 2. Here, we adopt a bandwidth for the $^{13}C^{18}O$ isotopomers, since they originally exhibit only one conformer and thus only one ν(CO) band. This means that the conformation of CO for the IDO-(L-Trp)-CO species is restricted as pointed out previously for IDO (*15*) and for tryptophan 2,3-dioxygenase (*29*). On the other hand, if we examine the ν(Fe−CO) mode, the frequency and shift values ($\Delta(^{13}C^{18}O)$) upon $^{13}C^{18}O$ substitution are 542 cm^{-1} ($\Delta(^{13}C^{18}O) = -17$ cm^{-1}), 522 cm^{-1} ($\Delta(^{13}C^{18}O) = -30$ cm^{-1}), and 531 cm^{-1} ($\Delta(^{13}C^{18}O) = -35$ cm^{-1}) for IDO-(L-Trp)-CO, IDO-CO, and IDO-(D-Trp)-CO, respectively. The isotopic shift value for IDO-(L-Trp)-CO is significantly small. This means that the vibrational displacement of the carbon atom of CO for the IDO-(L-Trp)-CO species is significantly smaller than that of the other two species based upon the relationship between the vibrational displacement and the frequency shift which occurs upon isotopic substitution (*30*). Since the absorption spectrum and most of the RR spectral patterns are similar (with the exception of the bands associated with CO of the IDO-(D-Trp)-CO species (Figures 1a and 2a) and those of the IDO-CO species (Figures 1b and 2b)), the binding of D-Trp to IDO-CO does not perturb the electronic and geometric structures of the porphyrin. It is notable that binding of D-Trp to IDO is confirmed by the frequency shifts of RR bands associated with CO under these experimental conditions. The frequency shifts are ascribed to a change in polarity of the heme pocket environment which is expected to occur upon binding of D-Trp. On the other hand, the absorption and RR spectral patterns of IDO-(L-Trp)-CO species (Figures 1c and 2c) are distinct from those of IDO-CO (Figures 1b and 2b). This means that binding of L-Trp significantly perturbs the electronic and geometric structure of the porphyrin. The characteristic features of IDO-(L-Trp)-CO include a higher ν(Fe−CO) frequency, a lower ν(CO) frequency, and an enhanced δ(FeCO) band. These characteristics have been reported for strapped heme model complexes (*31*). Taking these results into consideration, the carbon atom of CO sits very close to L-Trp, and this causes the vibrational displacement to be restricted. A hydrogen bond should exist between the O atom and L-Trp as indicated in a previous report (*15*). Under these conditions, the degree of Fe $d_\pi \rightarrow$ CO π^* back-donation is significant. This causes a decrease in the bond order of C−O (*20*, *31*). This is reflected in the low ν(CO) frequency at 1908 cm^{-1} for the L-Trp species relative to the other two species (Table 3). A positive polar environment enhances the back-bonding effect (*22*, *32*). This kind of geometry, in which O_2 is hydrogen-bonded to L-Trp, seems to be essential for the enzymatic reaction involving the IDO-(L-Trp)-O_2 complex and is favorable for cleavage of the O−O bond before incorporation of two oxygen atoms into Trp, to generate the ferryl-oxo intermediate (*10*, *11*). These effects are not seen for the IDO-(D-Trp)-CO species. The RR activation of the ν(OO) mode at 1138/1062 cm^{-1} (for $^{16}O_2/^{18}O_2$) for the oxygenated intermediate in the presence of L-Trp should be caused by similar geometry. This mode is not activated in the absence of L-Trp (*10*, *11*, *33*, *34*).

The sharp prominent Raman band at 328 cm^{-1}, assigned to the porphyrin γ_6 mode, is seen only for IDO-(L-Trp)-CO (Figure 2c) and not for IDO-CO and IDO-(D-Trp)-CO. This band was identified for the ferric cyanide complex but was not identified when the enzyme is in the reduced state (*15*). It is also seen for the ferryl-oxo intermediate and the oxygenated intermediate in the presence of L-Trp (330−332 cm^{-1}) (*34*) but not for the oxygenated intermediate in the absence of L-Trp (*11*). Thus, the band at 328 cm^{-1} could serve as a marker for the structure of the Fe-ligand moiety when L-Trp is bound. Under these conditions, deformation of the porphyrin plane occurs, and out-of-plane mode also becomes enhanced (*15*). Here, we note that this band is detectable not only for diatomic ligands such as CO, O_2, and CN^- but also for monatomic ligands such as O^{2-}. This might be an indication of an interaction of the Fe=O fragment with the L-Trp derivative during turnover.

The sharp bands at 1627 and 428 cm^{-1} for IDO-(L-Trp)-CO are ascribed to the ν(C=C) and $\delta(C_\beta-$vinyl) modes of the vinyl substituents (Figure 2c). The enhancement of the $\delta(C_\beta-$vinyl) mode at 421 cm^{-1} was previously reported for the IDO-(L-Trp)-O_2 ternary intermediate (*10*) and attributed to the movement of the vinyl groups with respect to the porphyrin plane (*15*). The ternary intermediate exhibits bands at 1629 and 422 cm^{-1} (*34*). These bands are very close to the bands observed for IDO-(L-Trp)-CO. The results are consistent with the occurrence of a conformational change of the vinyl groups with respect to the

heme plane, since the degree of conjugation of the π electrons between the vinyl C=C and the porphyrin is directly related to the RR enhancement. This makes the IDO-(L-Trp)-CO derivative a good model for the IDO-(L-Trp)-O_2 ternary intermediate. It is notable that the corresponding bands at 1626 and 423 cm^{-1} for IDO-(D-Trp)-CO and IDO-CO (Figure 2a,b) are not as sharp and prominent, relative to the corresponding bands at 1627 and 428 cm^{-1} for IDO-(L-Trp)-CO. Finally, it shoud be noted that the intensification of some of the Raman bands for IDO-(L-Trp)-CO is partially due to an increase in the Raman cross section, since the Soret absorption maximum shifts from 420 to 416 nm, closer to the excitation wavelength of 413.1 nm.

The ν(Fe−CO) frequency at 542 cm^{-1} for IDO-(L-Trp)-CO is identical at L-Trp concentrations of 100 μM and 10 mM. This means that the second "inhibitory" molecule of L-Trp does not bind to a position which is close to the first "substrate" molecule of L-Trp. This is consistent with the results reported for the oxygenated intermediate (*34*), where the ν(OO) and ν(Fe−O_2) frequencies were found to be independent of the concentration of L-Trp (50 μM versus 8 mM), although the X-ray structure shows a relatively large heme pocket.

The Enzymatic Activity for L-Trp and D-Trp. It has been reported that the K_m values of IDO for L-Trp and D-Trp are significantly different (0.02 mM vs ca. 5 mM for L- and D-Trp, respectively), but the V_{max} is of the same order (120 and 160 mol of Trp (mol of IDO)$^{-1}$ min^{-1} for L- and D-Trp, respectively) (*13*). However, these observations are inconsistent with the interpretations of the present work. The specific binding fashion of O_2 which involves significant interactions with Fe d_π and porphyrin π orbitals is essential for enzymatic activity. This specific interaction is seen only for IDO-(L-Trp)-CO. Although D-Trp does not induce such an interaction, as probed by Fe−C−O vibrational modes, V_{max} for D-Trp is similar to the V_{max} for L-Trp. This could be rationalized by the O−O bond of the IDO-(L-Trp)-O_2 ternary complex being favorably cleaved with the rate-limiting step occurring subsequently. On the other hand, in the IDO-(D-Trp)-O_2 ternary complex, the rate-limiting step is expected to be the O−O bond cleavage step. If the rates of the rate-limiting steps for IDO with bound L-Trp and D-Trp are close, the V_{max} for the two enantiomers would be expected to be similar.

The enzymatic activity assay was performed using ascorbate/methylene blue or NADH/cytochrome b_5 reductase/cytochrome b_5 as the reducing system. Thus, one might consider that the rate-limiting step could be different as a result of the intramolecular reaction in IDO and could represent an electron transfer step between the reductant and the mediator or between the mediator and IDO. However, since both the oxygenated and the ferryl-oxo intermediates are detectable when the reaction is initiated using IDO reduced with $Na_2S_2O_4$ (*11*), it is natural to consider that the rate-limiting step of *N*-formylkynurenine formation is represented by the rate of decay of either the oxygenated intermediate or the ferryl-oxo intermediate.

CONCLUSIONS

Binding of L-Trp but not D-Trp causes significant change in absorption spectra of IDO-CO. We have used vibrational signatures of CO as a probe to investigate the interaction between CO and Trp and have demonstrated a distinct CO binding fashion in IDO-(L-Trp) relative to IDO-(D-Trp) and substrate-free IDO. CO sits very close and is hydrogen-bonded to L-Trp and is constrained, so that the vibrational displacement is restricted. It has become evident that IDO-(L-Trp)-CO is a good model for IDO-(L-Trp)-O_2. Activation of O_2 to initiate the dioxygenation reaction should take place favorably through a binding mechanism in which back-bonding can provide overlap of the π electronic states of dioxygen with those of the porphyrin. The extent of back-bonding and the extent of steric constraint are significantly lower when D-Trp is bound to IDO. The different rate-limiting step for L-Trp and D-Trp reactions can account for the comparable V_{max}, although the extent of back-bonding in the ternary complex is different between these enantiomers. Significantly higher anharmonicity of the Fe−CO stretching oscillator of IDO, reflecting a specific heme environment, relative to that of oxygen carrier proteins might be responsible for the unique reactivity of the enzyme.

ACKNOWLEDGMENT

We thank Mr. Norihiro Okada for purifying the IDO samples.

REFERENCES

1. Yamazaki, F., Kuroiwa, T., Takikawa, O., and Kido, R. (1985) Human indolylamine 2,3-dioxygenase. Its tissue distribution, and characterization of the placental enzyme. *Biochem. J. 230*, 635–638.
2. Yamamoto, S., and Hayaishi, O. (1967) Tryptophan pyrrolase of rabbit intestine. D- and L-tryptophan-cleaving enzyme or enzymes. *J. Biol. Chem. 242*, 5260–5266.
3. Hayaishi, O., Rothberg, S., Methler, A. H., and Saito, Y. (1957) Studies on oxygenases. Enzymatic formation of kynurenine from tryptophan. *J. Biol. Chem. 229*, 889–896.
4. Mellor, A. L., and Munn, D. H. (2004) IDO expression by dendritic cells: tolerance and tryptophan catabolism. *Nat. Rev. Immunol. 4*, 762–774.
5. Takikawa, O. (2005) Biochemical and medical aspects of the indoleamine 2,3-dioxygenase-initiated L-tryptophan metabolism. *Biochem. Biophys. Res. Commun. 338*, 12–19.
6. Macchiarulo, A., Camaioni, E., Nuti, R., and Pellicciari, R. (2009) Highlights at the gate of tryptophan catabolism: a review on the mechanisms of activation and regulation of indoleamine 2,3-dioxygenase (IDO), a novel target in cancer disease. *Amino Acids 37*, 219–229.
7. Mellor, A. (2005) Indoleamine 2,3 dioxygenase and regulation of T cell immunity. *Biochem. Biophys. Res. Commun. 338*, 20–24.
8. Sono, M., Roach, M. P., Coulter, E. D., and Dawson, J. H. (1996) Heme-containing oxygenases. *Chem. Rev. 96*, 2841–2887.
9. Sugimoto, H., Oda, S., Otsuki, T., Hino, T., Yoshida, T., and Shiro, Y. (2006) Crystal structure of human indoleamine 2,3-dioxygenase: catalytic mechanism of O_2 incorporation by a heme-containing dioxygenase. *Proc. Natl. Acad. Sci. U.S.A. 103*, 2611–2616.
10. Lewis-Ballester, A., Batabyal, D., Egawa, T., Lu, C., Lin, Y., Marti, M. A., Capece, L., Estrin, D. A., and Yeh, S.-R. (2009) Evidence for a ferryl intermediate in a heme-based dioxygenase. *Proc. Natl. Acad. Sci. U.S.A. 106*, 17371–17376.
11. Yanagisawa, S., Yotsuya, K., Hashiwaki, Y., Horitani, M., Sugimoto, H., Shiro, Y., Appelman, E. H., and Ogura, T. (2010) Identification of the Fe−O_2 and the Fe=O heme species for indoleamine 2,3-dioxygenase during catalytic turnover. *Chem. Lett. 39*, 36–37.
12. Chung, L. W., Li, X., Sugimoto, H., Shiro, Y., and Morokuma, K. (2010) ONIOM study on a missing piece in our understanding of heme chemistry: bacterial tryptophan 2,3-dioxygenase with dual oxidants. *J. Am. Chem. Soc. 132*, 11993−12005.
13. Littlejohn, T. K., Takikawa, O., Truscott, R. J. W., and Walker, M. J. (2003) Asp274 and His346 are essential for heme binding and catalytic function of human indoleamine 2,3-dioxygenase. *J. Biol. Chem. 278*, 29525–29531.
14. Chen, Z., Ost, T. W. B., and Schelvis, P. M. (2004) Phe393 mutants of cytochrome P450 BM3 with modified heme redox potentials have altered heme vinyl and propionate conformations. *Biochemistry 43*, 1798–1808.
15. Terentis, A. C., Thomas, S. R., Takikawa, O., Littlejohn, T. K., Truscott, R. J. W., Armstrong, R. S., Yeh, S.-R., and Stocker, R. (2002) The heme environment of recombinant human indoleamine 2,3-dioxygenase. *J. Biol. Chem. 277*, 15788–15794.
16. Rajani, C., and Kincaid, J. R. (1998) Resonance Raman studies of hemoglobin with selectively deuterated hemes. A new perspective on

the controversial assignment of the Fe-CO bending mode. *J. Am. Chem. Soc. 120*, 7278–7285.
17. Tsubaki, M., Srivastava, R. B., and Yu, N.-T. (1982) Resonance Raman investigation of carbon monoxide bonding in (carbon monoxy) hemoglobin and -myoglobin: detection of iron-carbon monoxide stretching and iron-carbon-oxygen bending vibrations and influence of the quaternary structure change. *Biochemistry 21*, 1132–1140.
18. Lu, C., Lin, Y., and Yeh, S.-R. (2009) Inhibitory substrate binding site of human indoleamine 2,3-dioxygenase. *J. Am. Chem. Soc. 131*, 12866–12867.
19. Kerr, E. A., and Yu, N.-T. (1988) in Biological Applications of Raman Spectroscopy (Spiro, T. G., Ed.) Vol. III, Chapter 2, Wiley-Interscience, New York.
20. Li, X.-Y., and Spiro, T. G. (1988) Is bound carbonyl linear or bent in heme proteins? Evidence from resonance Raman and infrared spectroscopic data. *J. Am. Chem. Soc. 110*, 6024–6033.
21. Nagai, M., Yoneyama, Y., and Kitagawa, T. (1991) Unusual carbon monoxide bonding geometry in abnormal subunits of hemoglobin M Boston and hemoglobin M Saskatoon. *Biochemistry 30*, 6495–6503.
22. Ray, G. B., Li, X. Y., Ibers, J. A., Sessler, J. L., and Spiro, T. G. (1994) How far can proteins bend the FeCO unit? Distal polar and steric effects in heme proteins and models. *J. Am. Chem. Soc. 116*, 162–176.
23. Evangelistakirkup, R., Smulevich, G., and Spiro, T. G. (1986) Alternative carbon monoxide binding modes for horseradish peroxidase studied by resonance Raman spectroscopy. *Biochemistry 25*, 4420–4425.
24. Uno, T., Nishimura, Y., Tsuboi, M., Makino, R., Iizuka, T., and Ishimura, Y. (1987) Two types of conformers with distinct Fe-C-O configuration in the ferrous CO complex of horseradish peroxidase. Resonance Raman and infrared spectroscopic studies with native and deuteroheme-substituted enzymes. *J. Biol. Chem. 262*, 4549–4556.
25. Fesis, A., Rodriguez-Lopez, J. N., Thorneley, R. N. F., and Smulevich, G. (1998) The distal cavity structure of carbonyl horseradish peroxidase as probed by the resonance Raman spectra of His 42 Leu and Arg 38 Leu mutants. *Biochemistry 37*, 13575–13581.
26. Das, T. K., Friedman, J. M., Kloek, A. P., Goldberg, D. E., and Rousseau, D. L. (2000) Origin of the anomalous Fe-CO stretching mode in the CO complex of *Ascaris* hemoglobin. *Biochemistry 39*, 837–842.
27. Hirota, S., Ogura, T., and Kitagawa, T. (1995) Observation of nonfundamental Fe-O_2 and Fe-CO vibrations and potential anharmonicities for oxyhemoglobin and carbonmonoxyhemoglobin. Evidence supporting a new assignment of the Fe-C-O bending fundamental. *J. Am. Chem. Soc. 117*, 821–822.
28. Wang, J., Takahashi, S., and Rousseau, D. L. (1995) Identification of the overtone of the Fe-CO stretching mode in heme proteins: a probe of the heme active site. *Proc. Natl. Acad. Sci. U.S.A. 92*, 9402–9406.
29. Batabyal, D., and Yeh, S. R. (2007) Human tryptophan dioxygenase: a comparison to indoleamine 2,3-dioxygenase. *J. Am. Chem. Soc. 129*, 15690–15701.
30. Miyazawa, T. (1960) Normal vibrations of monosubstituted amides in the *cis* configuration and infrared spectra of diketopiperazine. *J. Mol. Spectrosc. 4*, 155–167.
31. Yu, N.-T., Kerr, E. A., Ward, B., and Chang, C. K. (1983) Resonance Raman detection of iron-carbonmonoxy stretching and iron-carbon-oxygen bending vibrations in sterically hindered carbonmonoxy "strapped hemes". A structural probe of iron-carbon-oxygen distortion. *Biochemistry 22*, 4534–4540.
32. Phillips, G. N., Jr., Teodoro, M. L., Li., T., Smith, B., and Olson, J. S. (1999) Bound CO is a molecular probe of electrostatic potential in the distal pocket of myoglobin. *J. Phys. Chem. B 103*, 8817–8829.
33. Yanagisawa, S., Yotsuya, K., Horitani, M., Sugimoto, H., Shiro, Y., Hashiwaki, Y., and Ogura, T. (2009) Detection of the iron-oxygen stretching Raman mode for human indoleamine 2,3-dioxygenase in the oxygenated form. *J. Biol. Inorg. Chem. 14* (Suppl. 1), S139–S152 (P168).
34. Yanagisawa, Y., Horitani, M., Sugimoto, S., Shiro, Y., Okada, N. , and Ogura, T. (2011) Resonance Raman study on the oxygenated and the ferryl-oxo species of indoleamine 2, 3-dioxygenase during catalytic turnover. *Faraday Discuss.* (DOI: 10.1039/c004552g).